Molecular Genetics and Metabolism Reports 25 (2020) 100664

Contents lists available at ScienceDirect

Molecular Genetics and Metabolism Reports

journal homepage: www.elsevier.com/locate/ymgmr

Case Report

Genome sequencing identifies a rare case of moderate Zellweger spectrum disorder caused by a *PEX3* defect: Case report and literature review

Whiwon Lee[a], Gregory Costain[a,b], Susan Blaser[c], Susan Walker[d], Christian R. Marshall[a,e,f], Hernan Gonorazky[g], Michal Inbar-Feigenberg[b,*]

[a] Centre for Genetic Medicine, The Hospital for Sick Children, Toronto, Ontario, Canada
[b] Division of Clinical and Metabolic Genetics, The Hospital for Sick Children, Toronto, Ontario, Canada
[c] Department of Diagnostic Imaging, The Hospital for Sick Children, Toronto, Ontario, Canada
[d] The Centre for Applied Genomics, The Hospital for Sick Children, Toronto, Ontario, Canada
[e] Genome Diagnostics, Department of Paediatric Laboratory Medicine, The Hospital for Sick Children, Toronto, Ontario, Canada
[f] Laboratory Medicine and Pathobiology, University of Toronto, Toronto, Ontario, Canada
[g] Division of Neurology, The Hospital for Sick Children, Toronto, Ontario, Canada

ARTICLE INFO

Keywords:
PEX3
Peroxisome biogenesis disorder
Zellweger spectrum disorder
Genome sequencing
Genetic testing

ABSTRACT

Defects in *PEX3* are associated with a severe neonatal-lethal form of Zellweger spectrum disorder. We report two moderately affected siblings whose clinical and biochemical phenotypes expand the reported spectrum of *PEX3*-related disease. Genome sequencing of an adolescent male with progressive movement disorder, spasticity and neurodegeneration, and previous non-diagnostic plasma very-long chain fatty acid analysis, revealed a homozygous likely pathogenic missense variant in *PEX3* [c.991G > A; p.(Gly331Arg)]. A younger sibling with significant motor decline since the age of three years was also subsequently found to be homozygous for the familial *PEX3* variant. A comprehensive review of the scientific literature identified three additional families with non-lethal infantile- or childhood-onset *PEX3*-related disease, which together with this clinical report illustrate the potential for highly variable disease severity. Our findings demonstrate the diagnostic utility of genome-wide sequencing for identifying clinically and biochemically heterogeneous inherited metabolic disorders such as the peroxisome biogenesis disorders.

1. Introduction

Peroxisome biogenesis disorders (PBDs; MIM 601539) are caused by variants in genes involved in peroxisomal assembly and function [1]. PBDs include Zellweger spectrum disorders (ZSDs) and rhizomelic chondrodysplasia punctata (RCDP) types 1 [2]. Classification of peroxisome biogenesis disorders in the Zellweger spectrum (PBD-ZSD), ranging from severe (ZS), intermediate (NALD), and mild (IRD) phenotypes, respectively. Individual clinical pictures are along a spectrum of disease severity and often do not fit into the original assigned categories. The extreme variability in disease manifestation ranging from onset of profound neurologic symptoms in newborns to progressive degenerative disease in adults presents practical challenges in disease diagnosis and medical management [2].

There are currently 13 peroxin genes associated with ZSDs [2]. Of these, *PEX3*, *PEX16*, and *PEX19* encode proteins involved in peroxisomal membrane protein (PMP) biogenesis [3]. Specifically, PEX3 is involved in PMP import and targeting [4,5]. The first three reported cases of PEX3 defect presented with a severe form of ZSD that resulted in early lethality [4,6–9]. While clinical heterogeneity was noted, all three patients shared dysmorphic facial features and severe neurologic findings in addition to clearly abnormal plasma and/or fibroblast very-long chain fatty acids (VLCFA) levels.

PEX3 defects are very rare [10]. A limited number of case reports have described patients with mild to moderate clinical presentations of ZSD who carried pathogenic variants in *PEX3*, suggesting there may be a broader clinical spectrum for *PEX3*-related disease [10–12]. Here we report two siblings with a clinically and biochemically nonspecific progressive neurological disorder of initially unclear etiology. Genome sequencing (GS) identified a homozygous likely pathogenic *PEX3*

Abbreviations: ES, exome sequencing; gnomAD, Genome Aggregate Database; GS, genome sequencing; IRD, infantile Refsum disease; NALD, neonatal adrenoleukodystrophy; MAF, minor allele frequency; PBD, peroxisome biogenesis disorder; PMP, peroxisomal membrane protein; RCDP, rhizomelic chondrodysplasia punctata; VLCFA, very-long chain fatty acids; X-ALD, X-linked adrenoleukodystrophy; ZSD, Zellweger spectrum disorder; ZS, Zellweger syndrome

* Corresponding author at: Clinical and Metabolic Genetics, The Hospital for Sick Children, 525 University Avenue, Toronto, ON M5G 1X8, Canada.
E-mail address: michal.inbar-feigenberg@sickkids.ca (M. Inbar-Feigenberg).

https://doi.org/10.1016/j.ymgmr.2020.100664
Received 6 July 2020; Received in revised form 9 October 2020; Accepted 10 October 2020

variant, confirming a diagnosis of ZSD. In addition to broadening the clinical spectrum of this rare disease, we use this case to demonstrate the diagnostic utility of GS as a first-line test for identifying clinically and biochemically heterogeneous inherited metabolic disorders.

2. Case report

The siblings were born to consanguineous parents. They were born at term by vaginal delivery with no complications after uneventful pregnancies. Neither had marked neonatal hypotonia nor dysmorphic features. The family reported no history of genetic, neurologic, or kidney diseases.

PI, a 17-year-old male, had normal development until approximately 18 months of age, when he presented with fever associated with ataxia and ophthalmoparesis. He had progressive developmental regression, ataxia, dysphagia and spasticity and by 13 years of age, had complete loss of ambulation and severe speech impairment. At age 16, he was admitted to the hospital with acute kidney injury, secondary to urinary tract obstruction. Neurological examination revealed horizontal and vertical nystagmus, abnormal smooth and saccadic eye movements, tremor, dystonia and spastic quadriplegia with multiple joint contractures, hyperreflexia and bilateral clonus. Ultrasound showed horseshoe kidneys with nephrocalcinosis and small non-obstructive stones. Imaged liver was normal in size and echotexture. Brain and C-T-L spine MRI at age's 2-years-11-months and 16-years showed diffuse progressive myelin and white matter loss with atrophy of brain and spinal cord (Fig. 1). Chromosomal microarray showed normal 46, XY results. Metabolic investigations (ammonia, lactate, venous blood gas, creatinine, electrolytes, liver enzymes, acylcarnitine profile, plasma amino acids, CDG, aryl-sulfatase and urine sulfatides, beta- galactosidase, galactocerebrosidase, total hexosaminidase and HEX−B, urine organic acids, homocysteine, copper, ceruloplasmin, free and total carnitine, and B12) were all normal. VLCFA analysis showed mild non diagnostic isolated elevation of C26:0 with minimal elevation of ratios: C24:C22 **1.009** (0.543–0.941 umol/L); C26:C22 **0.028** (0.005–0.017 umol/L); C26:1 0.757 (0.247–1.095 umol/L); C26:0 **1.090** (0.269–0.923 umol/L). A repeat analysis showed moderately elevated C26:C22 ratio but other indices were normal: C24:C22 0.918 (0.543–0.941 umol/L); C26:C22 **0.025** (0.005–0.017 umol/L); C26:1 0.634 (0.247–1.095 umol/L); C26:0 0.878 (0.269–0.923 umol/L). Again, this result was reported as non-diagnostic, however it was noted that adrenomyeloneuropathy or X-linked adrenoleukodystrophy could not be ruled out. As imaging studies (Fig. 1) and disease presentation in both male and female paediatric patients were not consistent with *ABCD1* mutation, GS was offered to this patient.

Sagittal T1W image (a) in Patient 1 at nearly 3 years of age demonstrates a normal size optic chiasm (small arrow), corpus callosum (arrow), brainstem and cerebellar vermis (long arrow). Sagittal T1W image (f) in Patient 2 at 12 years of age demonstrates loss of volume in all 3 structures. By 16 years of age in Patient 1 (k), the chiasm, corpus callosum (small arrow) and vermis (arrow) have significantly atrophied and there is enlargement of the basal cisterns. Early axial T2W image (b) in Patient 1 shows poor myelin maturation of the cerebellum (arrow) and increased T2 signal (short arrow) in the pontine tegmentum. Similar tegmental signal (g) is present in Patient 2 with the additional feature of cerebellar hemisphere atrophy (arrow). T2W axial image (l) in Patient 1 at 16 years shows further loss of pontine volume (black arrow) and marked enlargement of the interfoliate sulci (arrow).

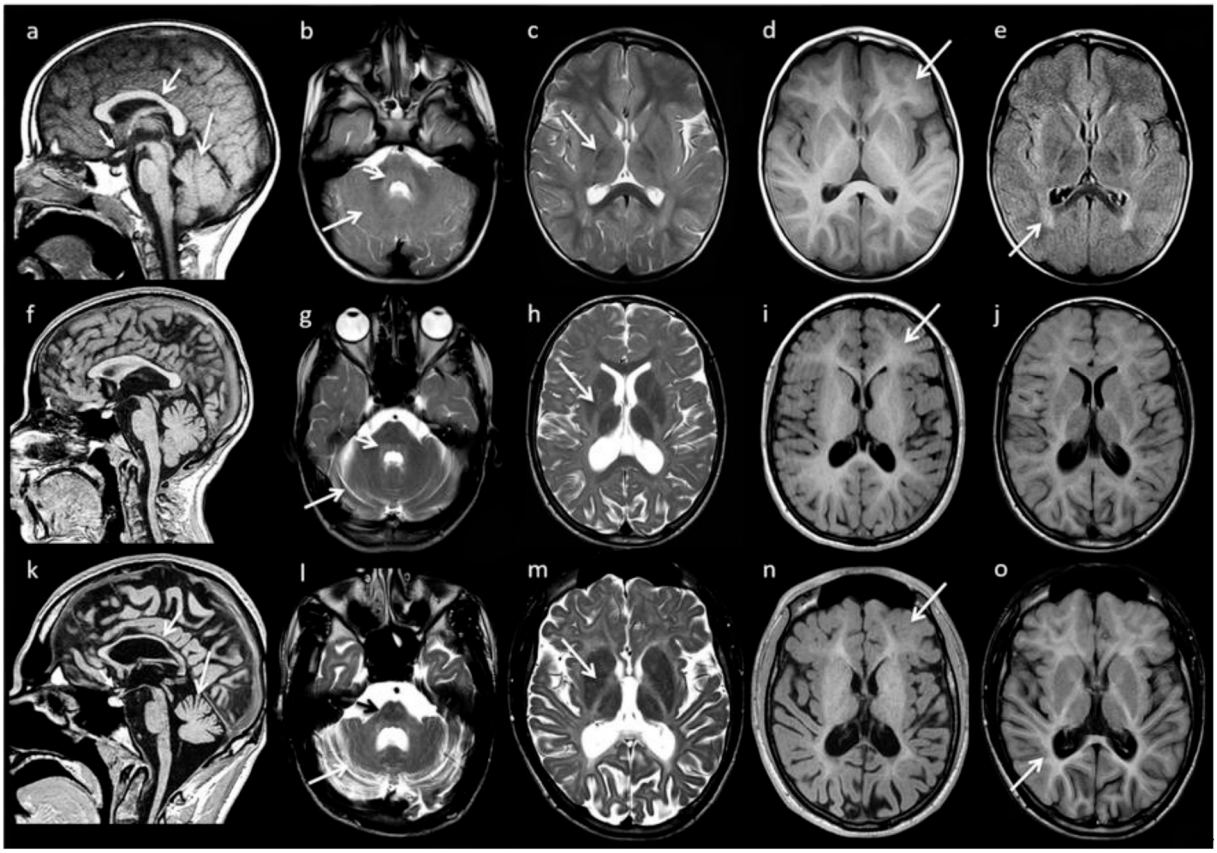

Fig. 1. Brain MRI of siblings with PEX3 mutation show progressive supra and infra-tentorial volume loss and progression of abnormal signal.
Patient 1, Top row (a-e): 2 years 11 months of age.
Patient 2, Middle row (f-j): 12 years.
Patient 1, Bottom row (k-o): 16 years.

Table 1
Biochemical studies.

	P1	P2	Normal Controls	X-ALD hemizygote	X-ALD Heterozygote	ZSD
Phytanic acid	0.420	0.410	< 3.00 μg/ml			
Pristanic acid	0.040	0.050	< 0.3 μg/ml			
				Mean ± 1SD		
C26:0 Hexacosanoic	**0.780** ▲	**0.690** ▲	0.23 ± 0.09	1.3 ± 0.45	0.68 ± 0.29	3.93 ± 1.50
C26:1	**0.620** ▲	**0.500** ▲	0.18 ± 0.09	0.34 ± 0.16	0.23 ± 0.10	4.08 ± 2.30
C24/C22	**1.165** ▲	**1.117** ▲	0.84 ± 0.10	1.71 ± 0.23	1.30 ± 0.19	2.07 ± 0.28
C26/C22	**0.042** ▲	**0.030** ▲	0.01 ± 0.004	0.07 ± 0.03	0.04 ± 0.02	0.50 ± 0.16
Plasmalogen/Fatty Acid ratios						
C16:0 DMA/C16:0 FA	0.085	0.096	0.103 (0.079–0.126)			
C18:0 DMA/C18:0 FA	0.196	0.216	0.241 (0.199–0.284)			

Early axial T2W image (c) in Patient 1 shows abnormally increased signal (arrow) surrounding the myelin stripe of the posterior limb of internal capsule. Over time in Patient 2 at 12 years (h) and Patient 1 at 16 years (m) abnormal signal replaces the myelin of the posterior (arrows) and anterior limbs of the internal capsule, there is diffuse loss of myelin signal and progressive enlargement of the ventricles and sulci. Normal T1 myelin signal (arrow) is present in Patient 1 on initial MRI (d), but is lost (arrows) by 12 years in Patient 2 (i) and 16 years in Patient 1 (n). FLAIR (e) shows abnormal signal in the posterior limb of internal capsule and periatrial white matter (arrow) in Patient 1. Abnormal signal extends to involve all white matter in Patient 2 (j) (arrow). Diffuse abnormal white matter signal and significant progression in central (arrow) and peripheral volume loss is seen by 16 years of age in Patient 1 image (o).

PII reached appropriate milestones until age 3 years, when she developed weakness in her legs and has subsequently experienced significant motor decline. This patient's brain MRI showed abnormal myelination at age 5 per her family's report. No records were available to confirm this information. At 12 years of age, she underwent additional MRI imaging showing diffusely abnormal white matter signal. On examination at age 11, the patient was alert and appropriate. She presented with dysarthria, dystonia and dysmetria. She had normal tone in upper limbs and scissoring posture with spasticity in lower limbs. She had contractures in both her ankles and knees and atrophy in thighs and calf muscles. She had multiple small café au lait spots (≤0.5 cm), pectus carinatum, and scoliosis. She used ankle and foot orthoses (AFOs) and was able to walk short distances with a walker.

Genome sequencing (GS) was performed at The Centre for Applied Genomics (Toronto, Canada) using DNA extracted from whole blood of the proband. Library preparation was performed from 500 ng of DNA using the Illumina TruSeq Nano DNA Library Prep Kit (omitting the PCR amplification step), followed by sequencing on the Illumina HiSeq X platform to generate paired-end reads of 150-bases in length. Sequence reads were mapped to the hg19 reference sequence using BWA v0.7.12. SNVs and indels were detected using GATK (v3.7). Detected variants were annotated using a custom pipeline based on ANNOVAR [13]. ERDS (Estimation by Read Depth with Single-nucleotide variants; Duke University) and CNVnator (Yale University) were used with a window size of 500 bp to detect copy number variants [14,15]. Structural variants were detected with Manta (v0.29.6) [16]. GS of PI identified a homozygous, likely pathogenic missense variant in the *PEX3* gene (NM_003630): c.991G > A (p.Gly331Arg). There were no pathogenic or likely pathogenic variants identified in other peroxisomal disorder genes.

Targeted Sanger sequencing of the variant for PII and the siblings' parents showed that PII was also homozygous, and that parents were heterozygous for this variant. This variant has been previously reported in a 9-year-old patient with moderate ZSD in the compound heterozygous state with a pathogenic variant [10]. This variant is reported in only two individuals in the heterozygous state (MAF = 0.000007964) in the Genome Aggregation Database (gnomAD) of 125,748 exomes and 15,708 genomes [17]. This residue is highly conserved across different species and this change is predicted as deleterious by SIFT, disease causing by MutationTaster and probably damaging by the PolyPhen-2 prediction software.

Upon identification of the *PEX3* defect, peroxisomal parameters and erythrocyte plasmalogen levels were studied in both siblings (Table 1). While the VLCFA levels were consistent with a defect in peroxisomal fatty oxidation, these levels were much lower than the levels that are diagnostic of ZS. Other parameters of PBDs were within normal range.

3. Discussion

We report two patients with moderate clinical presentation of ZSD due to a homozygous variant in *PEX3*, adding to the currently limited understanding of the disease spectrum associated with *PEX3* defects.

The original three patients with *PEX3* defects presented with the typical Zellweger phenotype that included dysmorphic facial features, severe neurologic findings, and early lethality [4,7–9]. All three patients carried variants that result in a premature termination of *PEX3* protein translation. In contrast, there is a lack of a clear pattern of clinical and biochemical presentations among less severely affected patients with *PEX3* variants. Table 2 provides a summary of the clinical and imaging findings of the mild to moderately affected patients. Except in one patient, who carries a nonsense variant and a missense variant, none of our and other reported mildly affected patients were described as having marked facial dysmorphisms.

The classical approach toward identification of patients with inherited metabolic diseases involves diagnostic algorithms that often begin with biochemical studies. We learn from our case and other published reports of patients with atypical presentations of PBDs that PBDs are extremely heterogeneous and it is difficult to delineate a clear clinical picture from which to base a reliable differential diagnosis. As the genotypic and phenotypic spectrum of inherited metabolic conditions expands, biochemical testing may not be sufficient for accurate diagnosis for heterogeneous inherited metabolic disorders. It is possible that PBDs are being underdiagnosed in less severely affected patients. While the value of biochemical studies should not be ignored, now with the availability of advanced molecular tools, comprehensive genetic testing should be integrated into the diagnostic system for PBDs. In Japan, a diagnostic system incorporating exome sequencing (ES) has led to an increase in the diagnosis of PBDs in patients with neurological diseases and atypical peroxisomal parameters [18].

In cases where biochemical studies show inconclusive results, GS is a time-efficient alternative to conventional biochemical and genetic testing strategies. It allows for the potential to detect all types of variants including structural and copy number variants as well as variants in regions not covered by ES (e.g., variants in non-coding regions and pseudogenes).

Our patients' diagnostic journey was long and complex. Despite having received an array of tests and medical assessments in several countries, the patient had not received an accurate diagnosis for

Table 2
Summary of clinical and imaging phenotypes our and published mild to moderately affected patients with PEX3 mutations.

Reference	This report		10	11	12	
	P1	P2			P1	P2
Sex	M	F	M	M	F	M
Ethnicity	Jordanian	Jordanian	NA	NA	Iraqi	Iraqi
Consanguinity	Yes		No	No	Yes	
Age at dx (yr)	17	11	9	32	26	22
Clinical Phenotype						
Onset	18 months	3 yr	8 months	1 yr 8 months	5 yr	"never been able to walk"
Initial presentation	Fever associated with ataxia and ophthalmo paresis	Weakness in legs	Psychomotor retardation, axial and peripheral muscular hypotonia, nephrocalcinosis	Unable to walk independently, spastic quadriplegia	Unable to walk, medical information from childhood sparse	Medical information from childhood sparse
Dysmorphic features	−	−	High forehead, posteriorly rotated low set ears	−	−	−
Neurological findings	Ataxia, spasticity, dysphagia	Dystonia, dysmetria	Severe spastic paraparesis, brisk reflexes with axial hypotonia, needed motor assistance using a wheelchair by age 4	Spastic quadriplegia,	Spastic tetraparesis, dysphagia	Spastic tetraparesis, dysphagia
Skeletal findings	scoliosis, pectus carinatum	scoliosis, pectus carinatum	NA	scoliosis with left convexity, thoracic kyphosis	NA	NA
Developmental delay / Intellectual disability	+	Requires education assistance, average grades, good communication abilities, good fine motor skills	NA	+	+	+
Speech impairment / Dysarthria	+	+	NA	+	+	+
Ophthalmological findings	Ophthalmoparesis, oculomotor apraxia, horizontal nystagmus	Visual fields normal extraocular movements were intact with interpreted pursuit.	Bilateral cataracts at age 4, nystagmus	Pallor of optic disc, no nystagmus	Nystagmus, visual impairment with severe myopia and papillary pallor	Visual impairment with hyperopia
Hearing impairment	NA	−	−	+	−	−
Neurogenic bladder	+	−	+	Renal cyst, renal hypertension	+	+
Seizures	−	−	+	−	−	+
Hepatosplenomegaly	−	NA	NA	−	−	−
Diagnostic Investigations						
MRI	Diffuse hypomyelination of brain and spine at age 16	MRI reported to show hypomyelination at age 5	MRI performed at 26 months, 3 and 4 yr were normal	Frontal lobe atrophy at age 23	Marked sulci with general atrophy, especially of the cerebellum, diffuse bilateral white matter hyperintensities on T2 and FLAIR, hypointense lesions in the basal ganglia and corticospinal tract bilaterally on T2-weighted images, radiological features consistent with leukodystrophy	
Plasma VLCFA						
C24:0/C22:0	Mildly elevated	Mildly elevated	Mildly elevated	Marked increase	NA	NA
C26:0/C22:0	Mildly elevated	Mildly elevated	Mildly elevated	Marked increase	NA	NA
C26:0	Mildly elevated	Mildly elevated	NA	NA	Normal	NA
Fibroblast C26:0	NA	NA	Mildly elevated	NA	NA	Normal
Karyotype analysis	46 XY normal	NA	46 XY normal	NA	NA	NA
Method of mutation detection	GS	Targeted Sanger Sequencing	Sequence analysis of *PEX* genes	Sequence analysis of *PEX* genes	ES	ES
Mutation	c.991G > A (p.Gly331Arg), homozygous	c.991G > A (p.Gly331Arg), homozygous	c.898C > T (p.Arg300*), c.991G > A (p.Gly331Arg)	c.1039G > T (p.Asp347Tyr), homozygous	c.206-1G > T, homozygous	c.206-1G > T, homozygous

Abbreviations: "-" = absent, "+" = present, yr = year, NA = not available or not reported, M = male, F = female, ES = exome sequencing, GS = genome sequencing, VLCFA = very-long chain fatty acids.

15 years. GS allowed for a hypothesis-free approach to evaluation of both candidate genes and variants types in the search for a diagnosis for our patient.

Timely and accurate diagnosis can not only change the management of the patient, but it also leads to subsequent testing and identification of at-risk family members. In our patient's family, an unaffected sibling will have the option to get carrier testing for future family planning.

GS has demonstrated superiority over conventional genetic testing strategies such as microarrays and next generation sequencing (NGS)-based multigene panels [19,20]. A recent study comparing the analytic and diagnostic performance of GS and ES demonstrated that GS has higher analytic performance than ES [21]. Additionally, GS has the ability to detect structural and copy number variants as well as variants in regions not covered by ES (e.g., variants in non-coding regions and pseudogenes). Thus, the diagnostic yield of GS is expected to increase as our ability to interpret the clinical significance of noncoding and structural variants improve [21]. A repeat VLCFA done for both patients after receiving the GS results showed levels were consistent with a defect in peroxisomal fatty oxidation supporting pathogenicity of the PEX3 c.991G > A variant.

In order to prevent significant diagnostic delays and its subsequent impact on the quality of care these patients receive, GS should be considered a first-line diagnostic test for patients with progressive developmental regression, non-specific VLCFA or peroxisomal parameters, and white matter changes on brain MRI.

PBDs are often difficult to diagnose due to their rarity and clinical and genetic heterogeneity. Timely diagnosis through the use of GS will allow families to receive appropriate care including but not limited to effective intervention for presenting symptoms, monitoring of disease progression, and genetic counselling.

4. Conclusion

This report illustrates the variable expression and severity of *PEX3*-related disease. Our findings demonstrate the diagnostic utility of GS for identifying clinically and biochemically heterogeneous inherited metabolic disorders.

Funding

This work was supported by funding from the Centre for Genetic Medicine at The Hospital for Sick Children (SickKids).

Author contributions

Conception, manuscript, preparation and revision of intellectual content: WL, GC, MI.

Acquisition of biochemical, genetic, and clinical data: GC, MI, SB, SW, CM, HG.

Review and critique, and final approval of the manuscript: WL, GC, MI, SB, SW, CM, HG.

Ethical approval

This case study was approved by the Research Ethics Board at SickKids as part of the Genome Clinic research (REB# 1000037726). Informed written consent was obtained from the patient's parents for the Genome Clinic research and specifically for publication of this case report.

Declaration of Competing Interest

The authors declare no potential conflicts of interest with respect to the research, authorship, and/or publication of this article.

References

[1] Shimozawa N. Peroxisomal Disorders, Peroxisomes: Biogenesis, Function, and Role in Human Disease, Springer, 2019, pp. 107–136.
[2] N. Shimozawa, T. Tsukamoto, T. Nagase, Y. Takemoto, N. Koyama, Y. Suzuki, et al., Identification of a new complementation group of the peroxisome biogenesis disorders and PEX14 as the mutated gene, Hum. Mutat. 23 (6) (2004) 552–558.
[3] S.J. Steinberg, G. Dodt, G.V. Raymond, N.E. Braverman, A.B. Moser, H.W. Moser, Peroxisome biogenesis disorders, Biochim. Biophys. Acta 1763 (12) (2006) 1733–1748.
[4] N. Shimozawa, Y. Suzuki, Z. Zhang, A. Imamura, K. Ghaedi, Y. Fujiki, et al., Identification of PEX3 as the gene mutated in a Zellweger syndrome patient lacking peroxisomal remnant structures, Hum. Mol. Genet. 9 (13) (2000) 1995–1999.
[5] M. Nakayama, H. Sato, T. Okuda, N. Fujisawa, N. Kono, H. Arai, et al., Drosophila carrying pex3 or pex16 mutations are models of Zellweger syndrome that reflect its symptoms associated with the absence of peroxisomes, PLoS One 6 (8) (2011) e22984.
[6] A. Poulos, J. Christodoulou, C.W. Chow, J. Goldblatt, B.C. Paton, T. Orii, et al., Peroxisomal assembly defects: clinical, pathologic, and biochemical findings in two patients in a newly identified complementation group, J. Pediatr. 127 (4) (1995) 596–599.
[7] A. Dursun, S. Gucer, M.S. Ebberink, S. Yigit, R.J. Wanders, H.R. Waterham, Zellweger syndrome with unusual findings: non-immune hydrops fetalis, dermal erythropoiesis and hypoplastic toe nails, J. Inherit. Metab. Dis. 32 (Suppl. 1) (2009) S345–S348.
[8] A.C. Muntau, P.U. Mayerhofer, B.C. Paton, S. Kammerer, A.A. Roscher, Defective peroxisome membrane synthesis due to mutations in human PEX3 causes Zellweger syndrome, complementation group G, Am. J. Hum. Genet. 67 (4) (2000) 967–975.
[9] K. Ghaedi, M. Honsho, N. Shimozawa, Y. Suzuki, N. Kondo, Y. Fujiki, PEX3 is the causal gene responsible for peroxisome membrane assembly-defective Zellweger syndrome of complementation group G, Am. J. Hum. Genet. 67 (4) (2000) 976–981.
[10] C. Maxit, I. Denzler, D. Marchione, G. Agosta, J. Koster, R.J.A. Wanders, et al., Novel PEX3 gene mutations resulting in a moderate Zellweger Spectrum disorder, JIMD Rep. 34 (2017) 71–75.
[11] S. Matsui, M. Funahashi, A. Honda, N. Shimozawa, Newly identified milder phenotype of peroxisome biogenesis disorder caused by mutated PEX3 gene, Brain and Development 35 (9) (2013) 842–848.
[12] K. Bjorgo, R. Fjaer, H.H. Mork, S. Ferdinandusse, K.D. Falkenberg, H.R. Waterham, et al., Biochemical and genetic characterization of an unusual mild PEX3-related Zellweger spectrum disorder, Mol. Genet. Metab. 121 (4) (2017) 325–328.
[13] A.C. Lionel, G. Costain, N. Monfared, S. Walker, M.S. Reuter, S.M. Hosseini, et al., Improved diagnostic yield compared with targeted gene sequencing panels suggests a role for whole-genome sequencing as a first-tier genetic test, Genet Med. 20 (4) (2018) 435–443.
[14] M. Zhu, A.C. Need, Y. Han, D. Ge, J.M. Maia, Q. Zhu, et al., Using ERDS to infer copy-number variants in high-coverage genomes, Am. J. Hum. Genet. 91 (3) (2012) 408–421.
[15] A. Abyzov, A.E. Urban, M. Snyder, M. Gerstein, CNVnator: an approach to discover, genotype, and characterize typical and atypical CNVs from family and population genome sequencing, Genome Res. 21 (6) (2011) 974–984.
[16] X. Chen, O. Schulz-Trieglaff, R. Shaw, B. Barnes, F. Schlesinger, M. Kallberg, et al., Manta: rapid detection of structural variants and indels for germline and cancer sequencing applications, Bioinformatics. 32 (8) (2016) 1220–1222.
[17] K.J. Karczewski, L.C. Francioli, G. Tiao, B.B. Cummings, J. Alföldi, Q. Wang, et al., The mutational constraint spectrum quantified from variation in 141, 456, Humans (2020) 531210 bioRxiv.
[18] S. Takashima, H. Saitsu, N. Shimozawa, Expanding the concept of peroxisomal diseases and efficient diagnostic system in Japan, J. Hum. Genet. 64 (2) (2019) 145–152.
[19] D.J. Stavropoulos, D. Merico, R. Jobling, S. Bowdin, N. Monfared, B. Thiruvahindrapuram, et al., Whole-genome sequencing expands diagnostic utility and improves clinical management in paediatric medicine, npj Genomic Medicine. 1 (1) (2016) 15012.
[20] G. Costain, S. Walker, M. Marano, D. Veenma, M. Snell, M. Curtis, et al., Genome sequencing as a diagnostic test in children with unexplained medical complexity, JAMA Netw. Open 3 (9) (2020) e2018109.
[21] S.F. Kingsmore, J.A. Cakici, M.M. Clark, M. Gaughran, M. Feddock, S. Batalov, et al., A randomized, controlled trial of the analytic and diagnostic performance of singleton and trio, rapid genome and exome sequencing in ill infants, Am. J. Hum. Genet. 105 (4) (2019) 719–733.